

Modeling the effects of climate change on hydrology and sediment load in a headwater basin in the Brazilian Cerrado biome



Vinícius Augusto de Oliveira^{a,b,*1}, Carlos Rogério de Mello^b, Samuel Beskow^a, Marcelo Ribeiro Viola^b, Raghavan Srinivasan^c

^a Hydrology and Hydrological Modeling in Watersheds Research Group, Federal University of Pelotas, Rua Gomes Carneiro, 01, Centro. Campus Porto – sala 212, CEP 96010-610 Pelotas, RS, Brazil

^b Water Resources Department, Federal University of Lavras, CP 3037, CEP 37200-000 Lavras, MG, Brazil

^c Spatial Sciences Laboratory, Department of Ecosystem Sciences and Management, Texas A&M University, 534 John Kimbrough Blvd., Room 305, College Station, TX 77843-2120, United States

ARTICLE INFO

Keywords:

Hydrological modeling
Sediment modeling
Regional Climate Model
Soil loss

ABSTRACT

The assessment of hydrological impacts due to a changing climate has been an important tool for supporting future planning and management actions to mitigate these impacts. This study aimed to assess the climate change impacts on streamflow and sediment loads in the Upper Paranaíba river basin (UPRB), Southeastern Brazil. The SWAT model was applied to estimate the streamflow and sediment loads under observed conditions and to quantify possible climate change impacts from a multi-model ensemble and four Regional Climate Models (RCM) under two climate change scenarios. The results showed that simulations from the RCMs indicated reductions in streamflow varying from 27.6 to 75%. In addition, the simulated sediment loads were in agreement with the temporal pattern of streamflow. Besides all the uncertainties involved in climate change impacts simulations, the UPRB would suffer serious problems regarding to the water availability in extreme climatic conditions. As this basin is entirely inserted on the Brazilian Cerrado biome, the results can be useful in the context of eco-hydrological services, such as fresh water availability and identification of the land-use/soil combinations that are more vulnerable to water erosion.

1. Introduction

The better understanding of the changes in streamflow and sediment loads and their potential driving forces is of paramount importance to effectively utilize and manage water resources (Li et al., 2016). Thus, climate change and human activities are the main forces that affect the hydrological processes and sediment transport in river basins (Milliman et al., 2008; Tang et al., 2011; Zhao et al., 2015).

Climate change is one of the most significant challenges that all living matters on the planet needs to face (Phan et al., 2011). According to the Fifth Assessment Report (AR5) of the International Panel on Climate Change (IPCC, 2013), climate change is a well-documented and acknowledged phenomenon, which is characterized by changes in climate patterns that are mainly driven by the increase of anthropogenic greenhouse gas concentration (Alexander et al., 2013).

It has been documented that climate change can cause a number of

environmental problems related to water resources and ecological services (IPCC, 2013; Cousino et al., 2015). In order to assess these impacts, hydrological models have been used as they have potential to provide reliable predictions of the quantity of runoff and sediment transport over time from land surface into streams, rivers and water bodies, thus supporting decision makers in developing watershed management plans for better soil and water conservation measures (Setegn et al., 2010). The use of hydrological models coupled with General Circulation Models (GCMs) and/or Regional Climate Models (RCMs) has been the most common approach to assess climate change impacts on streamflow (e.g. Dlamini et al., 2017; Molina-Navarro et al., 2015; Viola et al., 2014) and soil erosion (e.g. Lemann et al., 2016; Rodríguez-Blanco et al., 2016; Zhao et al., 2015).

Changes on runoff and streamflow can alter significantly the water availability, which directly impacts irrigation, urban water supply systems and hydropower production (de Oliveira et al., 2017; Viola

* Corresponding author.

E-mail addresses: aovinicius@gmail.com, viniciusaoliveira@yahoo.com.br (V.A. de Oliveira), samuel.beskow@ufpel.edu.br (S. Beskow), r.srinivasan@tamu.edu (R. Srinivasan).

¹ Present address: Universidade Federal de Lavras, Departamento de Recursos Hídricos, CP 3037, CEP 37200-000 Lavras, MG, Brazil.

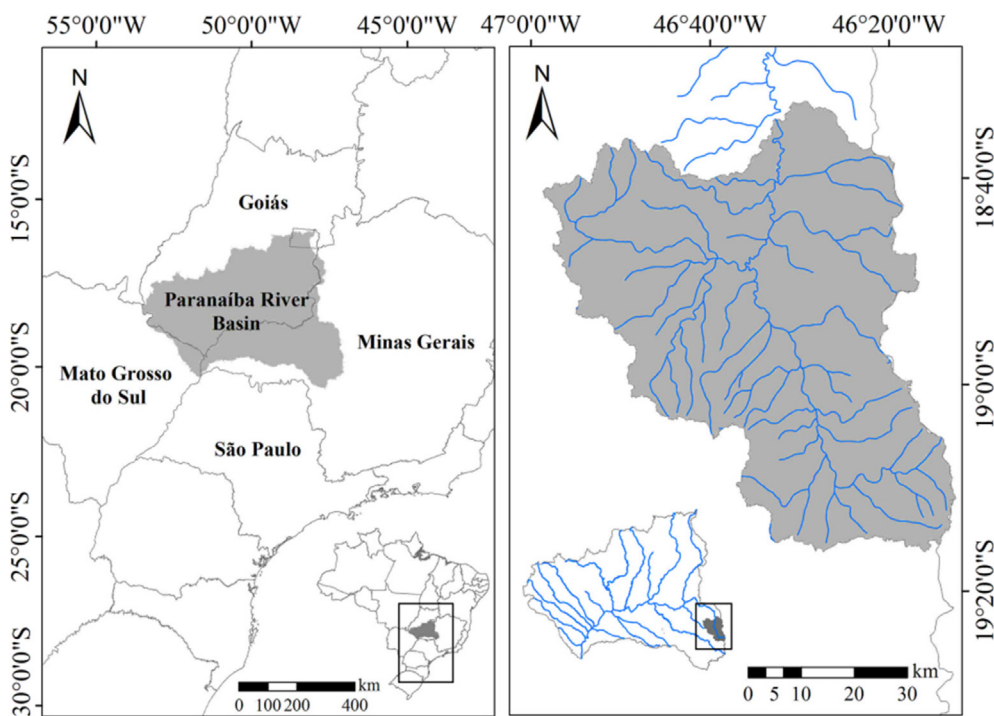


Fig. 1. Geographical location of the Upper Paranaíba River Basin.

et al., 2014). Changes in sediment load caused by water erosion (i.e. detachment of soil particles by rainfall and direct surface runoff) can result in a number of environmental problems, such as landslides, floods, loss of soil fertility, increase in pollutant transport, and siltation of water bodies and reservoirs (Jiang et al., 2007; Parajuli et al., 2016; Yan et al., 2013).

The Brazilian Cerrado biome, also referred to as Brazilian Savanna, encompasses an area of approximately 2 million km² in the central part of the country and is considered one of the world's environmental hotspots due to its biodiversity. The vegetation of the cerrado biome consists of forestlands, shrublands, grasslands, and wetland (Myers et al., 2000; Sano et al., 2010; Ferreira et al., 2011).

Brazil is strongly dependent on its water resources, which are used mainly for consumption, irrigation and electric energy production, making the country vulnerable to changes on rainfall patterns and hydrological regimes (de Oliveira et al., 2017). These characteristics are especially valid for the Cerrado biome, which is observed in the headwaters of some of the major rivers in South America, such as São Francisco, Paranaíba and Tocantins. Therefore, the assessment of potential climate change impacts on hydrology and sediment load is fundamental for a better understanding, planning and management of water resources under extreme climate in the Cerrado biome for the continued provision of its water resources and ecological services.

There are some studies conducted in Brazil regarding hydrological impacts linked with climate change. However, most of them were intended to investigate the impacts on runoff/streamflow and hydro-power potential (e.g. Mohor et al., 2015; Ribeiro Neto et al., 2016; de Oliveira et al., 2017; Viola et al., 2014). Thus, the impacts of climate change on river sediment load still need to be further investigated in Brazilian river basins, especially in a biome of great importance like the Cerrado.

The Paranaíba river is the second largest tributary of Paraná river basin, accounting for 25.4% of the total area and is entirely inserted in the Brazilian Cerrado biome, which has suffered serious anthropogenic impacts, especially due to agriculture and livestock activities. With an area of 222,800 km², the Paranaíba river basin is located in the Southeast/Central Brazil and has its drainage area in the states of Goiás

(63.3%), Minas Gerais (31.7%), Mato Grosso do Sul (3.4%) and the Federal District (1.6%). This basin has experienced constant economic development, especially with respect to the expansion of agricultural lands, mainly grains and sugar cane. Livestock production, mining and industrial activities are also relevant in this basin, impacting the Cerrado biome. In addition, the Paranaíba river basin is one of the most important basins in the country in regulating the streamflow for hydropower generation, with an installed capacity of approximately 8500 MW (ANA, 2013).

Given the importance of the Brazilian Cerrado biome regarding water availability and ecological services and the lack of studies investigating the hydrosedimentological behavior in function of climate change, this study aims to investigate the climate change impacts on hydrology and sediment load in a headwater basin of the Paranaíba river, located entirely within the Cerrado biome. For this purpose, the Soil and Water Assessment Tool (SWAT) was calibrated and validated on a monthly basis with respect to streamflow and sediment load of the Upper Paranaíba river basin. The climate change impacts were simulated over the 21st century (2007–2099) from four GCMs (HadGEM2-ES, MIROC5, BESM and CANESM2) and the ensemble procedure based on them, downscaled by the Eta Regional Climate Model under the Representative Concentration Pathways (RCP) 4.5 and 8.5.

2. Materials and methods

2.1. Study area characterization

The Upper Paranaíba river basin (UPRB) is located in the central-west of Minas Gerais State, entirely within the Brazilian Cerrado biome. For this study, a water level gauging station named "Patos de Minas" was defined to delimitate the basin, resulting in a drainage area of 3754 km² (Fig. 1).

According to the Köppen climate classification, the UPRB is characterized by the Aw type, a hot tropical climate characterized by two distinct seasons, wet and dry. (ANA, 2013). The mean annual precipitation is approximately 1480 mm, with 80% of it occurring between November and March. The mean annual temperature is 22 °C ranging

Table 1
K_{USLE} and C_{USLE} values.

Soil type	K _{USLE}	Reference
<i>K_{USLE} values</i>		
Latosol (Oxisol)	0.01913	Mannigel et al., (2002)
Cambisol	0.0508	Araújo et al. (2011)
Litholic Neosol	0.0569	Castro et al. (2011)
Land use	C _{USLE}	Reference
<i>C_{USLE} values</i>		
Agriculture	0.2	Land cover/plant growth SWAT database
Pasture	0.003	
<i>Cerrado</i>	0.003	
Native Forest	0.001	
Eucalyptus	0.001	
Bare soil	0.2	
Water	0	

from 16 and 28 °C, respectively, for the mean minimum and maximum temperatures.

The altitude in the UPRB ranges from 797 to 1309 m. The greatest precipitation depths occur in UPRB headwaters, where higher altitudes and the undulated relief contribute for the formation of orographic precipitation events (ANA, 2013). The available water in the basin is mainly used for irrigation, human consumption and for supplying the Emboreação hydropower plant, which presents an installed capacity of 1192 MW.

The vegetation of UPRB is predominantly Pasture (54.1% of the area), Savanna (*Cerrado*) (24.8%), Agriculture (14.2%) and Native Forest (*Mata*) (6.1%). Eucalyptus, bare soils and water bodies account for < 1% of the basin area. The soils in UPRB are Latosol (Oxisol), Cambisol and Litholic Neosol, which represent 76.2%, 21.3% and 1.4% of the basin area, respectively. Rock outcrop represents 1.1%.

2.2. Model description

The Soil and Water Assessment Tool (SWAT) is a large-scale model which was developed to predict the impact of land management practices on water, sediment and agricultural chemical yields in large complex watersheds with varying soils, land use and management conditions over long periods of time (Neitsch et al., 2005).

SWAT is a continuous-time, long-term, distributed-parameter, physically based hydrological model that divides the basin into sub-basins connected by a stream network. Each sub-basin is further delineated into small spatial units called hydrological response units (HRUs), which consist of lumped areas of unique combinations of land cover, slope and soil type (Arnold et al., 1998; Srinivasan et al., 2010).

The SWAT model simulates the hydrological cycle on a daily basis through water balance for each HRU in each sub-basin by quantifying the main hydrological processes, such as surface and subsurface flows, evapotranspiration, infiltration, percolation, and plant uptake. The water balance equation adopted by the SWAT model in each HRU is presented in Eq. (1).

$$SW_t = SW_0 + \sum_{i=1}^t (P_{day} - Q_{surf} - E_a - w_{seep} - Q_{gw}) \quad (1)$$

where SW_t is the final soil water content (mm), SW₀ is the initial soil water content on day i (mm), t is the time (days), P_{day} is the amount of precipitation on day i (mm), Q_{surf} is the amount of surface runoff on day i (mm), E_a is the amount of evapotranspiration on day i (mm), w_{seep} is the amount of water entering the vadose zone from the soil profile on day i (mm), and Q_{gw} is the amount of base flow on day i (mm).

SWAT calculates the daily surface runoff using either the SCS Curve Number procedure (CN-SCS) (USDA-SCS, 1972) or Green-Ampt infiltration method (Green and Ampt, 1911). The peak flow is calculated by a modified rational method and the potential evapotranspiration can

be calculated by the Penman-Monteith (Allen et al., 1998), Priestley and Taylor (1972) or Hargreaves et al. (1985) methods. In this study, the CN-SCS and the Penman-Monteith methods were adopted.

Erosion and sediment yield are simulated by the Modified Universal Soil Loss equation (MUSLE) (Williams, 1995) for each HRU as follows:

$$E = 11.8 \cdot (Q_{surf} \cdot q_{peak} \cdot A_{hru})^{0.56} \cdot K_{USLE} \cdot C_{USLE} \cdot P_{USLE} \cdot LS_{USLE} \cdot CFRG \quad (2)$$

where E is the sediment yield on a given day (Mg), Q_{surf} is the surface runoff volume (mm·ha⁻¹), q_{peak} is the peak direct surface runoff rate (m³ s⁻¹), A_{hru} is the area of the HRU (ha). K_{USLE} is the USLE soil erodibility factor (MJ mm ha⁻¹ h⁻¹ yr⁻¹), C_{USLE} is the USLE cover and management factor, and P_{USLE} is the USLE support practice factor and varies from 0 to 1. As most of the watershed has no erosion control practices, the P factor was considered to be equal to 1 (Durães et al., 2016; de Oliveira et al., 2014). LS_{USLE} is the USLE topographic factor and CFRG is the coarse fragment factor.

In this study, the values of K_{USLE} and C_{USLE} were obtained from the literature as these factors have been well studied and documented. The adopted values are showed in Table 1.

A detailed description of the SWAT and MUSLE models can be found in Arnold et al. (1998), Srinivasan et al. (1998) and Neitsch et al. (2005).

2.3. Model setup

2.3.1. Hydro-meteorological and spatial data

For the model setup, SWAT requires input data for land use, soil and topography. The land use map was obtained based on Landsat 8 images from 2013 with the aid of supervised classification through the maximum likelihood classifier. The soil map was derived from the Minas Gerais State Environmental Foundation (FEAM, 2010) on a scale of 1:650,000. For topography information, the ASTER Digital Elevation Model (DEM) was used in a spatial resolution of 30 m.

The SWAT model also requires hydro-meteorological daily data such as maximum and minimum temperatures, humidity, solar radiation and wind speed. These data were obtained from weather stations of the Brazilian National Institute of Meteorology (INMET) to estimate the evapotranspiration. In addition, data sets related to precipitation and streamflow were obtained from the Brazilian National Water Agency (ANA-Hidroweb).

Fig. 2(a) shows the spatial distribution of the precipitation, streamflow and weather gauges stations used to calibrate SWAT with respect to streamflows, as well as the data points for the climate projections from the Regional Climate Models (RCMs) used in this study. Fig. 2(b) and (c) depict the land use and soil maps, respectively.

2.3.2. Sediment data

In order to calibrate the SWAT model for estimation of sediment loads in the UPRB, suspended sediment concentration time series were obtained from the Minas Gerais Water Resources Institute (IGAM). These data were used to fit the sediment-discharge rating curve, which relates suspended solid discharges (Q_{ss}, Mg day⁻¹) to the respective discharges (Q, m³s⁻¹) at the measuring section (Eq. (5)). Mean monthly sediment loads were then obtained from discharge series using the sediment-discharge rating curve represented by Eq. (5) (Fig. 3).

$$Q_{ss} = 0.059 \times Q^{2.3034} \quad (5)$$

This methodology was adopted since sediment-discharge rating curves has been successfully applied in previous studies in regions with scarce sediment data, such as those conducted by Durães et al. (2016), Shrestha et al. (2016) and Naik and Jay (2011).

2.4. Calibration, validation and model performance evaluation

The calibration and uncertainty analyses for SWAT simulations

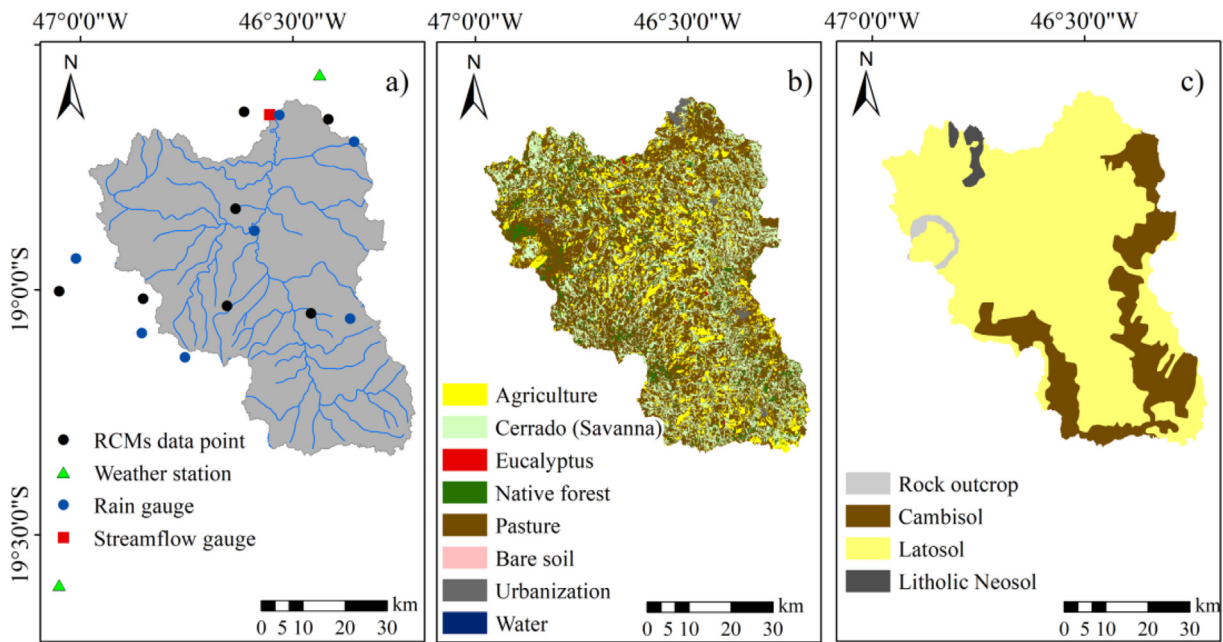


Fig. 2. Hydrologic, pluviometric, weather stations and RCMs grid point (a), land use (b) and soil (c) maps of the Upper Paranafba River Basin.

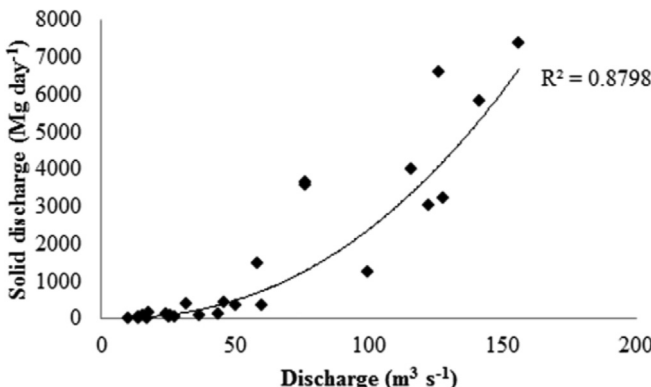


Fig. 3. Sediment rating curve from Patos de Minas gauge station.

were carried out in SWAT-CUP, which is a stand-alone software capable of dealing with SWAT output text files. Also, it integrates different optimization algorithms, such as SUFI-2 (Abbaspour et al., 2004), GLUE (Beven and Binley, 1992), ParaSol (van Griensven and Bauwens, 2003) and Markov Chain Monte Carlo (MCMC). Among them, the Sequential Uncertainty Fitting (SUFI-2) algorithm stands out due to its capability to account for all sources of uncertainty within the parameter ranges, e.g. uncertainty in driving variables, conceptual model, parameters, and measured data (Abbaspour et al., 2007).

Automatic calibration through SUFI-2 was performed using a monthly streamflow series (1993–2001) from the “Patos de Minas” streamflow gauging station. The validation was performed updating the SWAT model with the parameters obtained in the calibration and compared against the observed hydrograph (2002–2007). The warm-up period was considered from 1990 to 1992. Calibration and validation of sediment load was performed manually after streamflow validation was done.

To evaluate the SWAT performance with respect to the calibration and validation periods, two commonly used precision statistical measures were considered: the Nash-Sutcliffe Efficiency (NSE) (Nash and Sutcliffe, 1970) and the percent bias (PBIAS), which were calculated according to Eqs. (5) and (6), respectively.

$$\text{NSE} = 1 - \left[\frac{\sum_{i=1}^n (Q_{\text{obs}_i} - Q_{\text{sim}_i})^2}{\sum_{i=1}^n (Q_{\text{obs}_i} - Q_{\text{mean}_i})^2} \right] \quad (6)$$

$$\text{PBIAS} = \left[\frac{\sum_{i=1}^n (Q_{\text{obs}_i} - Q_{\text{sim}_i})}{\sum_{i=1}^n (Q_{\text{obs}_i})} \right] \times 100 \quad (7)$$

where Q_{obs} , Q_{sim} and Q_{mean} are the observed, simulated and mean streamflow, respectively.

The evaluation criteria considered in this study was proposed by Moriasi et al. (2007): “Very good” ($\text{NSE} > 0.75$; $\text{PBIAS} < \pm 10$), “Good” ($0.65 < \text{NSE} < 0.75$; $\pm 10 < \text{PBIAS} < \pm 15$), “Satisfactory” ($0.50 < \text{NSE} < 0.65$; $\pm 15 < \text{PBIAS} < \pm 25$) and “Unsatisfactory” ($\text{NSE} < 0.50$; $\text{PBIAS} > \pm 25$).

For sediment load, simulations are classified as “Very good” ($\text{PBIAS} < \pm 15$), “Good” ($\pm 15 < \text{PBIAS} < \pm 30$), “Satisfactory” ($\pm 30 < \text{PBIAS} < \pm 55$) and “Unsatisfactory” ($\text{PBIAS} > \pm 55$).

2.5. Future climate projections

In this study, the simulations of the future climate were derived from four General Circulation Models (GCMs) HadGEM2-ES, MIROC5, BESM and CANESM2 dynamically downscaled by the RCM Eta/CPTEC. All these models were run over South America with a spatial resolution of 20 km (Chow et al. 2014a). Additionally, an ensemble of the models was also used to simulate the future climate as a measure to reduce the uncertainties of the projections. Importantly, we used these models as they were calibrated and downscaled using the same RCM (Eta/CPTEC) with outputs in an adequate spatial resolution for hydrological purposes (20 km), being the ones available for the studied region with these characteristics. Dynamical downscaling methods use GCM variables as boundary conditions to drive a nested Regional Circulation Model with higher spatial and temporal resolution that simulates regional climate processes and orographic influence (Shamir et al., 2015). In this sense, the downscaling methods provide more adequate and feasible projections for the use of hydrological watershed scale models.

The downscaling method provided simulations covering the following periods: 1961–2005 (baseline); 2007–2040; 2041–2070; and 2071–2099 (Chou et al., 2014a,b). The variables simulated by the models used to assess the potential hydrological impacts of the UPRB were daily precipitation and daily maximum and minimum

temperatures. The temperatures were used to estimate future evapotranspiration rates. Relative humidity, wind speed and solar radiation were determined from the weather generator in SWAT model, in which daily values for weather are generated from average monthly values.

The downscaled models (Eta-GCMs) were simulated based on two different Representative Concentration Pathways (RCPs) – RCP 4.5 and RCP 8.5, which are based on the anthropogenic and non-anthropogenic radiative forcings (4.5 and 8.5 W m⁻², respectively) by the end of the 21st century.

The projections obtained from the downscaled models were part of a bilateral effort developed under the Climate Change Policy Program (PoMuC), an initiative of the Brazilian government, coordinated by the Ministry of the Environment (MMA), within the context of the Sustainable Development Cooperation between Brazil and Germany, within the framework of the International Initiative for the Protection of Climate (IKI) of the Federal Ministry for the Environment, Nature Protection, Construction and Nuclear Safety (BMUB) of Germany (PROJETA, 2018). These projections were chosen for this study because the Eta model better represent the climate of South America (Chou et al., 2014a), especially in Brazil, where this model has been used for regional forecast (Pesquero et al., 2009).

Although RCMs are more reliable to reproduce the regional climate, they are still subjected to systematic errors when comparing the simulated climate at the reference period to the same period's observations, as they are numerical models (Chen et al., 2013). Thus, bias correction of the RCM output for hydrologic impact assessment is highly recommended (Graham et al., 2007; Teutschbein and Seibert, 2010). Bias correction is a statistical approach that seeks to use information from biased model outputs (Chen et al., 2013). For this study, the linear scaling method for precipitation and temperature was adopted. A detailed description of the method can be found in studies such as Lenderink et al. (2007) and Teutschbein and Seibert (2012). Applications of this method can be found in studies such as de Oliveira et al. (2017), Fiseha et al. (2014) and Teutschbein and Seibert (2012).

In order to perform the climate simulation, the closest RCM points from the actual rain gauges and meteorological stations were selected to calibrate SWAT model to UPRB, as recommended by Cousino et al. (2015) (Fig. 2). After performing the bias correction, monthly streamflow simulations from the baseline period (1961–2005) were compared to those from the three future time periods (2007–2040, 2041–2070 and 2071–2099) with respect to the assessment of the impacts on hydrology and sediment load in UPRB.

3. Results and discussion

3.1. Calibration and validation of the SWAT model

3.1.1. Streamflow

The SWAT model was calibrated and validated using monthly streamflow data from "Patos de Minas" gauging station (Fig. 2a). For simulation, 3 years were considered for warm-up (1990–1992), 9 years for calibration (1993–2001) and 6 years for validation (2002–2007). Relative to calibration, 14 parameters associated with the surface and subsurface runoff were used. In validation, these parameters were updated in SWAT with the values of the best simulation obtained during the calibration phase. Then, the model performed simulations with these calibrated parameters for the respective validation periods. Table 2 illustrates the parameter descriptions, initial ranges and the final calibrated values of the best simulation generated in calibration for UPRB.

Fig. 4 depicts the observed and simulated hydrograph (a), the scatter plot (b) and the flow duration curves (FDC) (c) of the observed and simulated streamflows. The results in Fig. 4a indicates that the model was able to simulate the monthly streamflow for both calibration and validation periods, capturing most of the peaks and adequately

simulated the recession periods. In addition, the results presented in Fig. 4b and c confirm the good performance of SWAT for UPRB in monthly time step, allowing to infer that the observed and simulated streamflows are linearly and closely related.

Also, the statistical coefficients for performance evaluation showed that the simulated streamflows had a good agreement in relation to the observed ones, resulting in NSE of 0.89 and 0.93 for calibration and validation, respectively, and percent bias (PBIAS) of -4.5 and -3.5%, respectively, for calibration and validation. Thus, the SWAT model had a "very good" performance for either the calibration and validation periods, as NSE was greater than 0.8 and PBIAS was within the range of $\pm 10\%$ (Moriasi et al., 2007).

3.1.2. Sediment load

The calibration of the sediment loads in the UPRB was performed after calibration and validation of streamflows by means of manual calibration. In order to improve the model's accuracy for streamflow and sediment load simulations, manual calibration has been employed in several studies (Ma et al., 2014; Ouyang et al., 2015; Zhang et al., 2015). For this calibration, 5 parameters regarding hydrosedimentology (transport and deposition) were used (Table 2). Validation was performed according to the procedure aforementioned for streamflow validation.

Fig. 5 presents the observed and simulated sediment loads for the calibration (a) and validation (b) periods. The results showed that SWAT model, for both calibration and validation periods, was able to simulate monthly sediment loads from UPRB, with mixed signals during the wet season (October to March), alternating between under and overestimation of the peaks, especially during calibration. Regarding the dry period (April to September), the simulation culminated in overestimation in relation to the observed data for both calibration and validation periods.

The statistical coefficients for performance evaluation showed that the simulated sediment load presented NSE of 0.67 and 0.63, respectively, for calibration and validation, and percent bias (PBIAS) of -29 and 25.8%, respectively, for calibration and validation. According to the evaluation criterion proposed by Moriasi et al. (2007), the SWAT model presented "Good" ($0.65 < \text{NSE} < 0.75$) and "Satisfactory" ($0.50 < \text{NSE} < 0.65$) performance when estimating sediment loads regarding the NSE, for calibration and validation, respectively. Considering the PBIAS, SWAT presented a "good" ($\pm 15\% < \text{PBIAS} < \pm 30\%$) performance for both calibration and validation periods.

Fig. 6 illustrates the accumulated sediment load during the analyzed period. It can be noted that the accumulation of the simulated sediment loading is greater than the observed, mainly due to the overestimation during the dry period. However, the accumulation of the observed and simulated sediment loads converges to approximately 100.10^5 Mg by the end of the simulated period (2007).

As sediment is transported mainly during flooding events, it is important to stress that the model was able to accurately estimate the peak flows, especially in the wettest months, as also obtained by Zeiger and Hubbart (2016). It has been reported in the literature the difficulty of hydrological models to accurately capture peak flows, especially during the validation period. This can be attributed to model structures and datasets used (Beskow et al., 2016; Mello et al., 2008).

However, the results of this study showed a good agreement between the simulated and observed peak flows, except for the wet period of 2006–2007 when there was a greater underestimation of the peak sediment load. This may be due to uncertainty in the Modified Universal Soil Loss Equation (MUSLE), which tends to overestimate and underestimate, respectively, small events and large events of precipitation/streamflow (Jackson et al., 1986; Johnson et al., 1986). This can also be related to the uncertainties in both sediment sampling and sediment-discharge rating curve, especially if there are peak flows in the series higher than the flows used to obtain such rating curve (Tomkins, 2014).

Table 2

Parameters used to calibrate UPRB as well as their ranges and final values.

Parameter	Parameter description	Initial range		Final Value
		Max	Min	
<i>Streamflow parameters</i>				
v_ESCO	Soil evaporation compensation Coefficient	0.5	0.95	0.71
r_CN2	Initial SCS runoff curve number for moisture condition II	-0.1	0.1	-0.099
v_ALPHA_BF	The baseflow recession constant	0.005	0.015	0.009
a_GW_DELAY (days)	Groundwater delay time	-30	60	-17.02
a_GWMN (mm)	Threshold depth of water in the shallow aquifer required for return flow to occur	-1000	1000	-982.52
v_CANMX (mm)	Maximum canopy storage	0	30	16.87
v_CH_K2 (mm h^{-1})	Effective hydraulic conductivity in main channel	0	10	8.58
v_CH_N2	Manning's "n" value for the main channel	-0.01	0.2	0.036
v_EPCO	Plant uptake compensation factor	0.01	1	0.511
v_GW_REVAP	Groundwater "revap" Coefficient	0.02	0.2	0.032
a_REVAPMN (mm)	Threshold depth of water in the shallow aquifer for "revap" or percolation to the deep aquifer to occur	-1000	1000	-262
r_SOL_AWC (mm mm^{-1})	Soil available water capacity	-0.05	0.05	-0.0495
r_SOL_K (mm h^{-1})	Saturated hydraulic conductivity	-0.05	0.05	0.0267
v_SURLAG	Surface runoff lag coefficient	0.01	24	3.68
<i>Sediment parameters</i>				
v_ADJ_PKR	Peak rate adjustment factor for sediment routing in the subbasin (tributary channels)	0.5	2	1.15
v_SPCON	Linear parameter for calculating the maximum amount of sediment that can be reentrained during channel sediment routing.	0.0001	0.001	0.00085
v_SPEX	Exponent parameter for calculating sediment reentrained in channel sediment routing	1	1.5	1.28
v_CH_COV1	Channel erodibility factor	0	1	0.1
v_CH_COV2	Channel cover factor	0	1	0.12

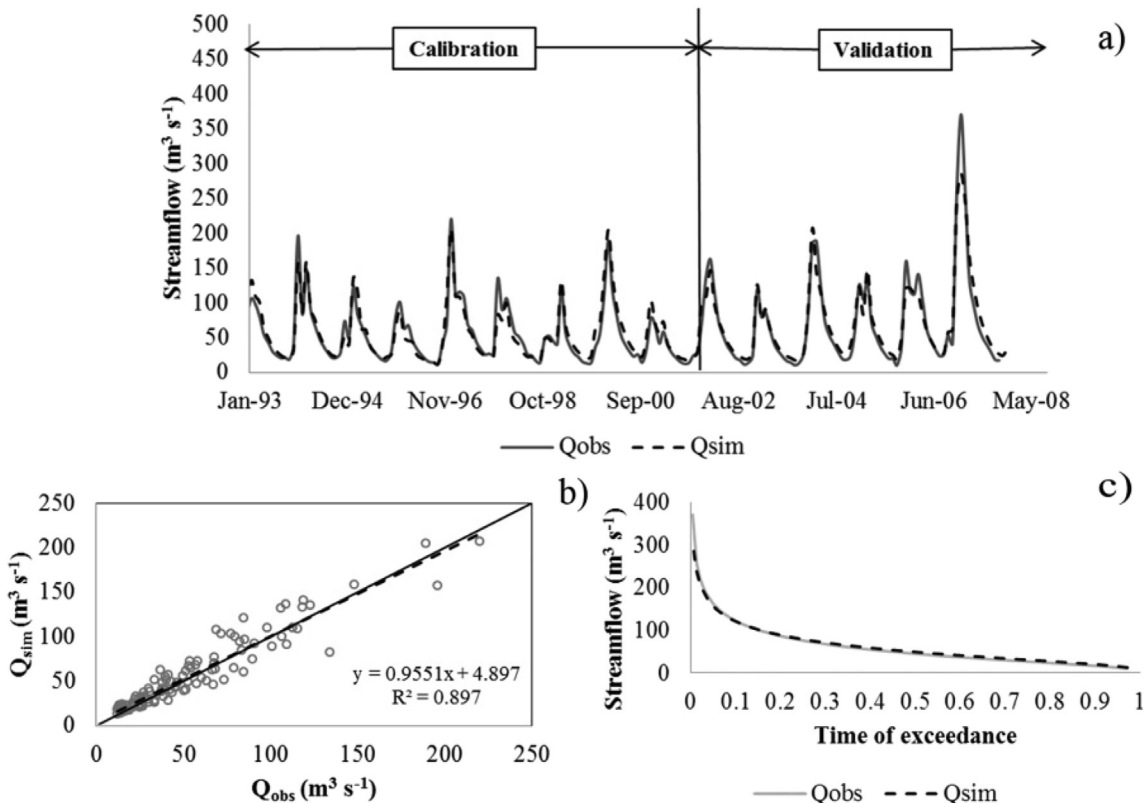
Prefixes 'v', 'r' and 'a' correspond to the operations 'replace', 'relative' and 'add', respectively.

3.2. Climate change projections

Climate change projections of monthly precipitation and maximum and minimum temperatures after bias correction in each period analyzed for the ensemble of RCMs under the RCPs 4.5 and 8.5 are presented in Fig. 7. Changes in mean annual precipitation and maximum and minimum temperatures throughout the 21st century from the

multi-model ensemble and each RCM are presented in Table 3.

The multi-model ensemble projections presented increases for both mean maximum and minimum temperatures throughout the 21st century. Under the RCP 4.5, the multi-model ensemble simulations showed an average increase of 2.0 °C for both maximum and minimum temperatures, whereas under the RCP 8.5 presented an average increase of 3.0 and 3.1 °C. Increases in maximum temperature varied from 1.4 °C

Fig. 4. Observed and simulated monthly streamflows (a), $Q_{\text{obs}} \times Q_{\text{sim}}$ scatter plot (b) and Observed and simulated flow duration curves (c) from the UPRB.

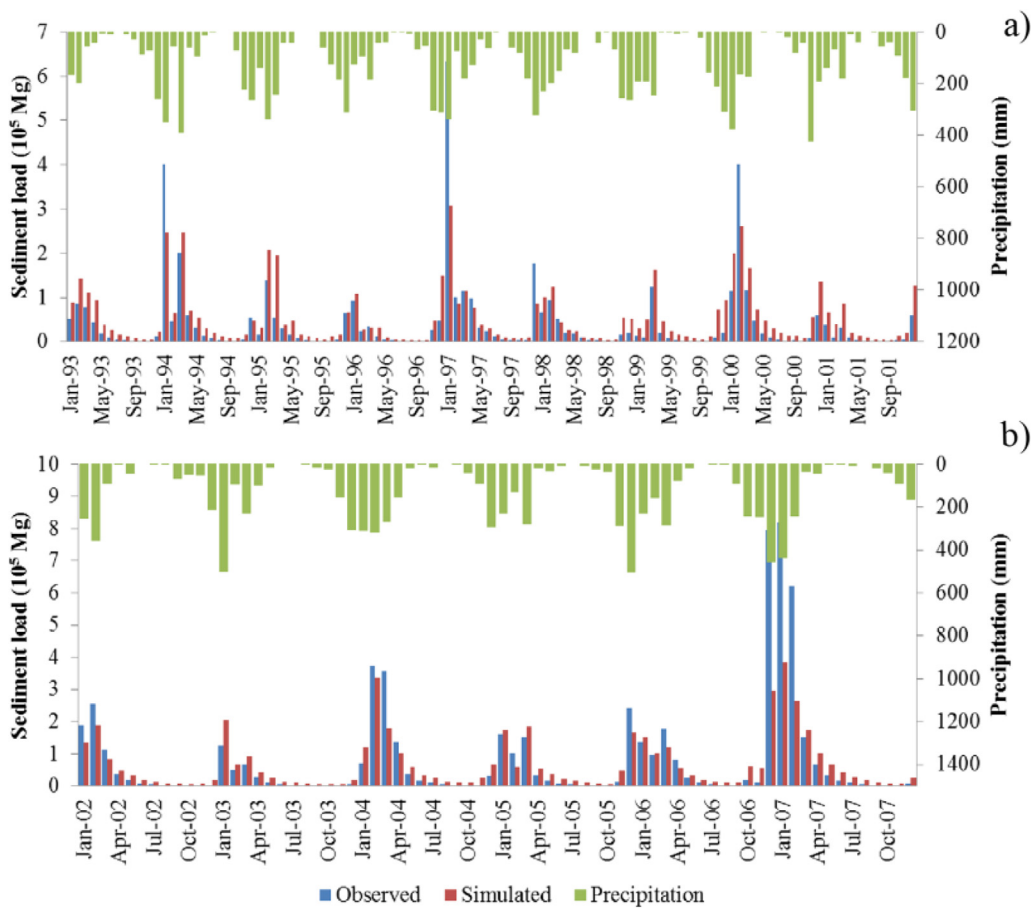


Fig. 5. Observed and simulated monthly sediment loads for the calibration (a) and validation (b) periods from the UPRB.

(Eta-BESM) to 2.8 °C (Eta-HadGEM2-ES) under the RCP 4.5 and 2.2 °C (Eta-BESM) and 3.9 °C (Eta-HadGEM2-ES) under the RCP 8.5. For the minimum temperature, the increases ranged from 1.7 °C (Eta-BESM) to 2.6 °C (Eta-CANESM) under the RCP 4.5 and 2.2 °C (Eta-BESM) and 3.9 °C (Eta-HadGEM2-ES) under the RCP 8.5.

Regarding the precipitation, the ensemble projections showed, for the entire future period (2007–2099), reductions of 13.5 and 14.5% for the RCPs 4.5 and 8.5, respectively, meaning an amount of annual precipitation up to 279.9 mm. The reductions simulated by the RCMs varied from 16.7% (Eta-BESM) to 28.1% (Eta-HadGEM2-ES) under the

RCP 4.5 and from 14.5% (Eta-MIROC5) to 37.2% (Eta-HadGEM2-ES) under the RCP 8.5.

According to Chou et al. (2014a), the Eta-HadGEM2-ES is more sensitive to the increase of greenhouse gases. The major warming tends to occur in Central and Southeast Brazil, independently of the GCM or RCP, where a high-densely populated area and high economic activities are observed.

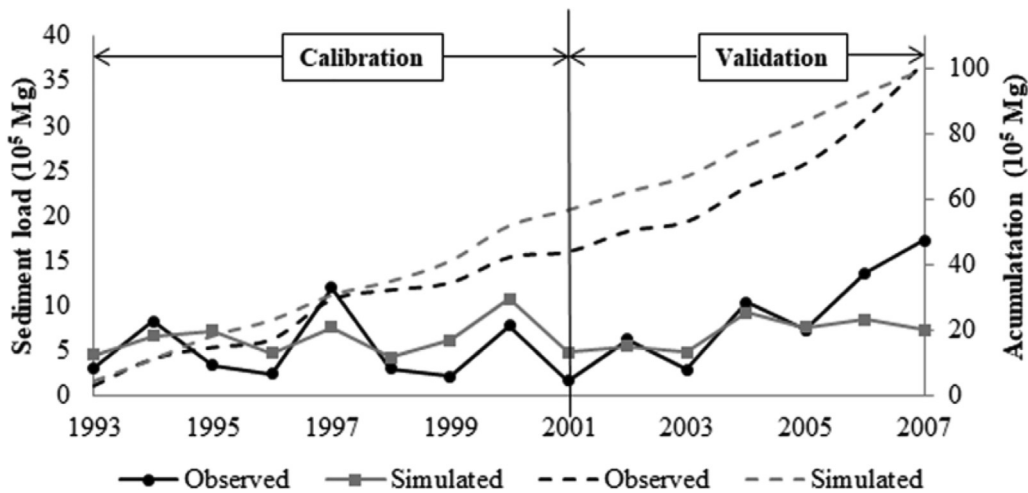


Fig. 6. Observed and simulated annual sediment load from the UPRB.

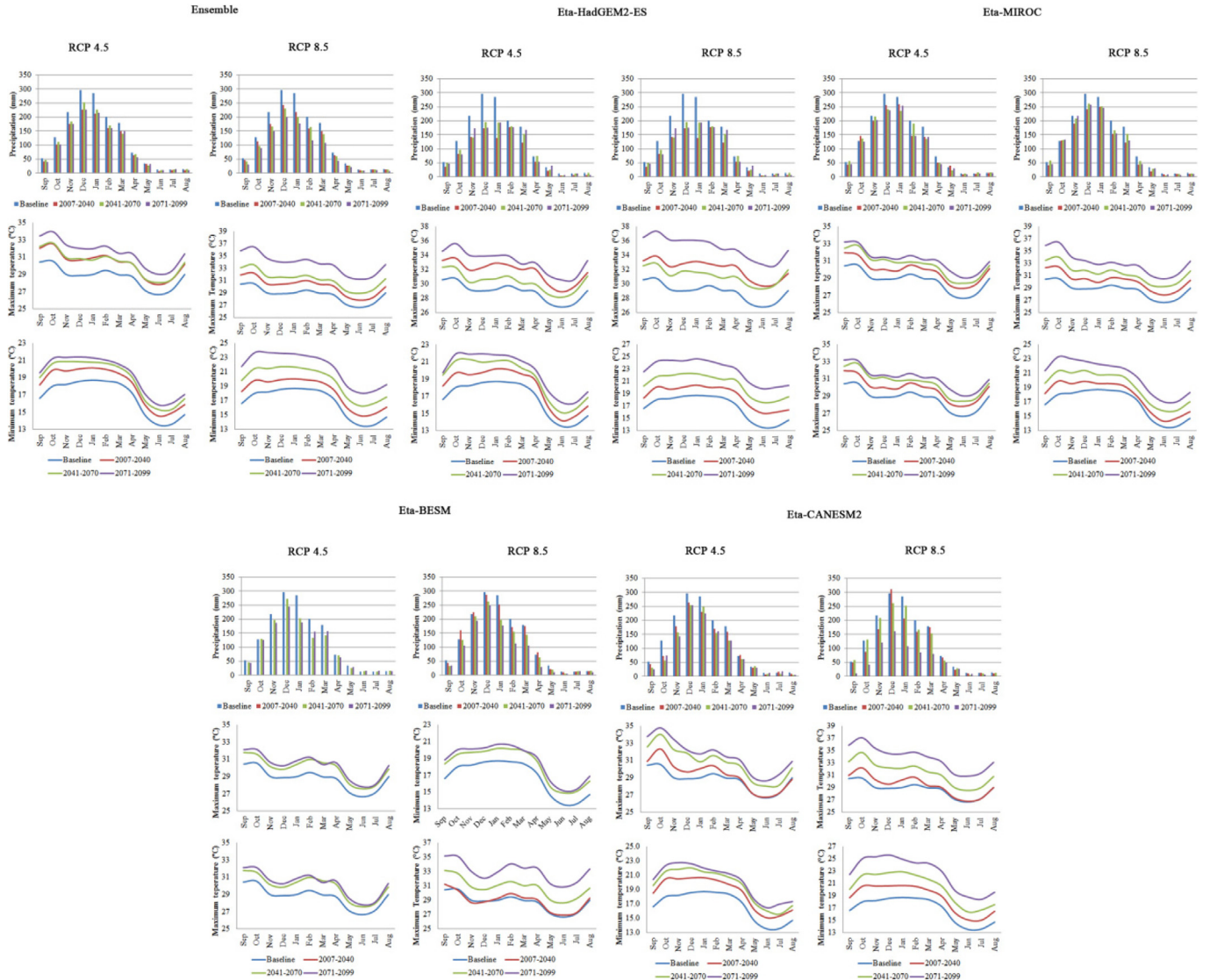


Fig. 7. Mean monthly climate change projections (precipitation and maximum and minimum temperatures) for the UPRB from the multi-model ensemble and the RCMs Eta-HadGEM2-ES, Eta-MIROC5, Eta-BESM and Eta-CANESM2 under RCP 4.5 and RCP 8.5 scenarios.

Table 3

Changes in mean annual precipitation and maximum and minimum temperatures throughout the 21st century from the multi-model ensemble and the RCMs Eta-HadGEM2-ES, Eta-MIROC5, Eta-BESM and Eta-CANESM2 under RCP 4.5 and RCP 8.5 scenarios.

Model	Δ Precipitation (%)		Δ Maximum temperature (°C)		Δ Minimum temperature (°C)	
	RCP 4.5	RCP 8.5	RCP 4.5	RCP 8.5	RCP 4.5	RCP 8.5
Ensemble	−13.5	−14.5	2	3	2	3.1
Eta-HadGEM2-ES	−28.1	−37.2	2.8	3.9	2.2	3.9
Eta-MIROC5	−13.5	−14.5	1.8	2.8	1.6	2.5
Eta-BESM	−16.7	−16.8	1.4	2.2	1.7	2.2
Eta-CANESM2	−21.5	−33.3	1.8	2.8	2.6	3.8

3.3. Climate change impacts over UPRB

3.3.1. Hydrological impacts

Fig. 8 presents the mean monthly streamflow projections simulated by the SWAT model coupled with the multi-model ensemble and the aforementioned RCMs. Although a wide range of uncertainties is noted

in the magnitude of the changes, a general decreasing trend in streamflow can be highlighted for all RCMs and their respective ensemble.

The mean monthly streamflow was overestimated during the baseline period for both wet and dry periods and for all the RCMs, with mean errors varying from 44 to 54%. Similar results were obtained by de Oliveira et al. (2017), using SWAT model and the RCMs Eta-HadGEM2 and Eta-MIROC5, and Viola et al. (2014), using LASH model and the Eta-HadCM3, both found mean errors varying from 12 to 41%, for the Upper Grande River Basin.

According to Teutschbein and Seibert (2010), the differences between observed and simulated streamflow in climate change impacts assessments are common since the use of the RCM data as inputs are generally not able to satisfactorily reproduce observed long-term seasonal streamflow, presenting deviations both in timing and magnitude. Also, according to Chen et al. (2013), even using bias-corrected precipitation data, the use of GCMs combined with RCMs for hydrological impact assessments can be unable to reproduce adequately observed streamflows in some cases.

This behavior of the models can be attributed to various uncertainties existent in climate change studies, such as GCM/RCM model structures, emission scenarios, parameterization, downscaling methods

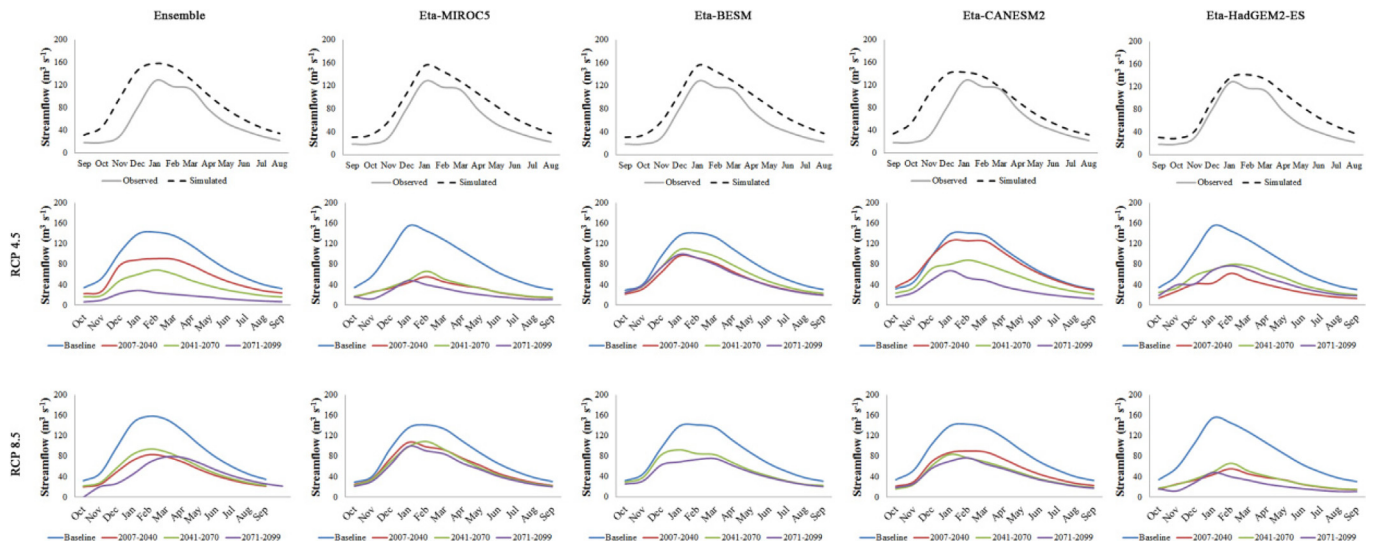


Fig. 8. Mean monthly streamflow simulations from the multi-model ensemble and the RCMs Eta-HadGEM2-ES, Eta-MIROC5, Eta-BESM and Eta-CANESM2 for the UPRB, under the RCP 4.5 and RCP 8.5.

and uncertainties related to the hydrological models (Kay et al., 2009). According to Vetter et al. (2017), the GCMs are the largest sources of uncertainties in hydrological impact studies, followed by the emission scenarios and hydrological models. Regarding the hydrological models, in the case of the present study, we can observe a very good performance of the SWAT to simulate monthly streamflow, allowing to state that uncertainties from this source are reduced.

With respect to downscaling methods, Prudhomme and Davies (2009) reported that these techniques are important sources of uncertainty. In a similar study, Fowler and Ekström (2009) concluded that the largest contribution to uncertainty in the multi-model ensembles comes from the boundary conditions used by the RCMs.

In addition, the choice of the bias-correction method plays an important role in climate change impact studies. According to Chen et al. (2013), bias-correction methods somewhat improve the RCM-simulated precipitation in the representation of streamflow, however, they are unable to improve the coherence between modeled and observed time series (Chen et al., 2013).

Furthermore, this study adopted a linear scaling of temperature and precipitation to correct the bias in the datasets generated by the RCMs. The linear scaling method is the simplest bias correction method, which simply adjusts the mean monthly values based on the differences between the observed and RCM-simulated data, neglecting the correction of the wet-day frequency and intensity of heavy rainfall events. Generally, the RCMs tend to overestimate the occurrence of wet days with small amount of rainfall, which is commonly known as “drizzle effect” (Chen et al., 2013; Fowler et al., 2007; Teutschbein and Seibert

2012).

The multi-model ensemble followed the same pattern as the RCMs, presenting intra-annual reductions varying from 27.6 to 75%. Greater decreases occurred mainly in the wet period, between October and March, with mean reduction of 44.4% and 52.3% for the RCPs 4.5 and 8.5, respectively, throughout the 21st century. The hydrological impacts were more pronounced during 2071 to 2099, under the RCP 8.5, with reductions in the peak flows of up to 75%. Thus, a notorious problem with water availability can be expected for the Brazilian Cerrado watersheds, with severe impacts for the environment and the economy.

With respect to the RCMs, the simulations from SWAT forced by the RCMs Eta-HadGEM2-ES and Eta-CANESM2 presented greater hydrological impact when compared to the other RCMs. The reductions of streamflow during the wet period ranged from 27.8 to 84.3%, independently of the RCP considered. This was expected since these RCM estimated greater reductions in precipitation and higher increases in temperatures. The RCMs Eta-MIROC5 and Eta-BESM presented lesser impacts on streamflow when compared to the others, with reductions varying from -6.4 to 64.6% in the wet period, independently of the RCP considered. Regardless of the RCMs or RCPs, the results showed that the water budget over the Brazilian Cerrado region would be negatively affected by the changes in climate projected by the models.

These patterns of reductions can also be observed in the mean annual streamflow projected by the multi-model ensemble and the RCMs projections, which are presented in Fig. S1 in the Supplementary material.

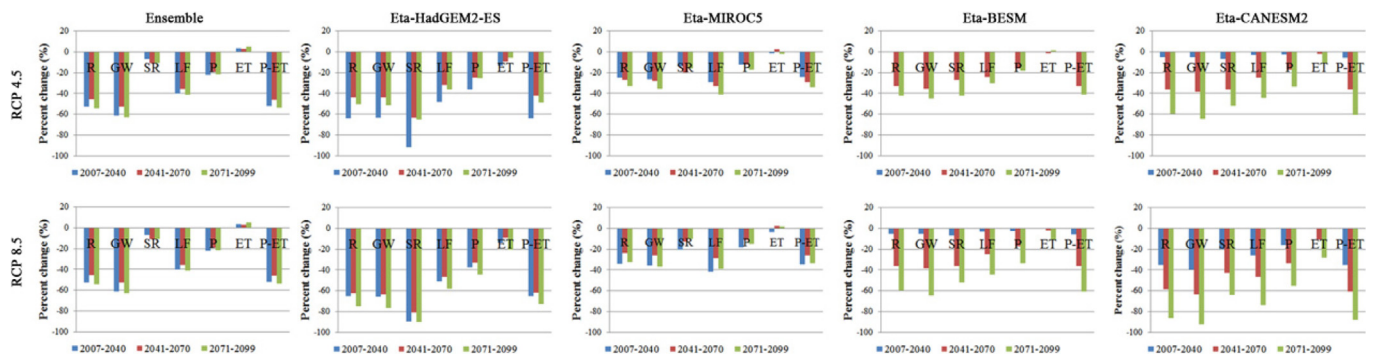


Fig. 9. Mean annual water balance simulated by the multi-model ensemble and the RCMs Eta-HadGEM2-ES, Eta-MIROC5, Eta-BESM and Eta-CANESM2 for the UPRB under the RCP 4.5 and RCP 8.5.

The mean annual water balance projections are presented in Fig. 9, which shows the percent changes of the future time periods in relation to the baseline (1961–2005) for the components total runoff (R), groundwater (GW), surface runoff (SR), lateral flow (LF), precipitation (P), evapotranspiration (ET) and P-ET, which represent the water surplus for the hydrological processes in the land-phase of the hydrological cycle.

According to the multi-model ensemble projections, the vertical water balance (P-ET), which indicates the availability of water for the surface hydrology, has presented significant decreases, showing values of up to 81.6% by the end of 2099, under the RCP 8.5. This implicates in serious hydrological impacts for Brazilian Cerrado throughout the 21st century, compromising the agriculture, hydro-electricity, urban supply and for the environment in general. Also, the components R, GW, LF and SR were projected to decrease for both RCP 4.5 and 8.5 as a result of the reduction of the vertical water balance. These results show that, similarly to the streamflow projections, the simulations using SWAT forced by Eta-HadGEM2-ES and Eta-CANESM2 presented greater reduction of the water balance components when compared to the Eta-MIROC5 and Eta-BESM.

3.3.2. Hydrosedimentological impacts

Fig. 10 depicts the mean monthly sediment loads simulated based on the multi-model ensemble, the RCMs, RCPs and time periods. In general, the simulations indicated a reduction in the peak sediment load during the wet period, especially between November and February, following the same trends of streamflow.

The multi-model ensemble projections indicated reductions of the peak sediment loads ranging from 17.8 to 51.9% under the RCP 4.5 and 28.3 to 71.3% under the RCP 8.5 throughout the century. In general, the changes of the sediment loads would follow the trends of the streamflow (Phan et al., 2011), however, our results presented mixed signals, especially considering the dry period for the RCMs Eta-HadGEM2-ES and Eta-MIROC5. The results of the Eta-HadGEM2-ES simulations for the dry period indicate an increase in the sediment loads from 8.9 to 85.3% under the RCP 4.5, between April to August, and an increase ranging from 5.4 to 45.8% under the RCP 8.5. The Eta-MIROC5 simulations presented increases in the dry period varying from 27.3 to 233.6% under the RCP 4.5 and 6 to 243.1% under the RCP 8.5.

According to Shrestha et al. (2013, 2016), the changes in sediment loads in response to climate change will not always happen in the same direction than streamflow, thereby suggesting that the sediment load projections are more sensitive to changes in temperature and rainfall than streamflow.

An increase on the sediment loads during a period where the runoff is reduced can be further explained by the water stress of the plants, which is caused by a reduction of the precipitation and an increase of the temperature. This would increase the transpiration of the vegetation, thus reducing the amount of biomass (Shrestha et al., 2016;

Trenberth et al., 2000). Therefore, unprotected soils will be more vulnerable to soil loss during rainfall events. Also, the extreme climate could lead to an increase of the rainfall intensity, which, combined with the reduced soil cover, may lead to an increase in the sediment yield at an event-based scale (Cousino et al., 2015; Shrestha et al., 2016). All these features are especially important since during the dry period the soils in Cerrado region are normally not cultivated, becoming the surface yet more exposed to the rainfall.

The results of the annual sediment load changes for the multi-model ensemble, RCMs, RCPs and time periods are presented in Table 4. In general, the annual sediment loads simulated by the multi-model ensemble presented decreases ranged from a 33.3 to 55.2%.

Regarding the RCMs, the annual sediment loads simulated by the Eta-HadGEM2-ES and Eta-CANESM2 presented the greater reductions, ranging from 28.4 to 79.7%. The Eta-BESM projections presented moderate reductions, varying from 7.4 to 59.1%, whereas the Eta-MIROC5 presented mixed signals, projecting increases from 2.6 to 12.8% during the periods of greater increases in the temperatures (2041–2070 for the RCP 8.5 and 2071–2099 for both RCPs 4.5 and 8.5) and decreases of up to 21.7% during the first time period (2007–2040) under the RCP 8.5.

Similar results were found by Cousino et al. (2015), who studied the climate change impacts in streamflow and nutrients of the Maumee River watershed, located in the Great Lakes Region (USA). They reported that the moderate climate change scenarios would reduce the annual runoff (up to –24%) and sediment yield (up to –26%), while a greater extreme scenario would result in a smaller runoff reduction (up to –10%) and an increase in sediment (up to 11%). Also, investigating the climate change impacts on streamflow and sediments in the Mekong River Basin using various climate models outputs, Shrestha et al. (2013) found changes in the annual sediment yield varying from –26.9 to 158.5% and mean monthly sediment yield ranging from –81 to 207.3%.

This study may provide useful information for future planning and management of natural resources and provide support in the implementation of strategies to mitigate the effects of climate change in the region. As the sub-basins of the Paranaíba River basin present similar climate conditions and is entirely within the Cerrado biome with similar land-uses, soils and management, the results of this study may be used to predict the hydrological behavior and sediment loads of data-scarce watersheds within the Paranaíba River basin through parameter transferring. In addition, this study may support future ecological impacts studies in the Cerrado biome, especially in the improvement of the methodological approach.

4. Conclusions

The SWAT model was calibrated and validated with respect to streamflows and sediment loads from the Upper Paranaíba River Basin

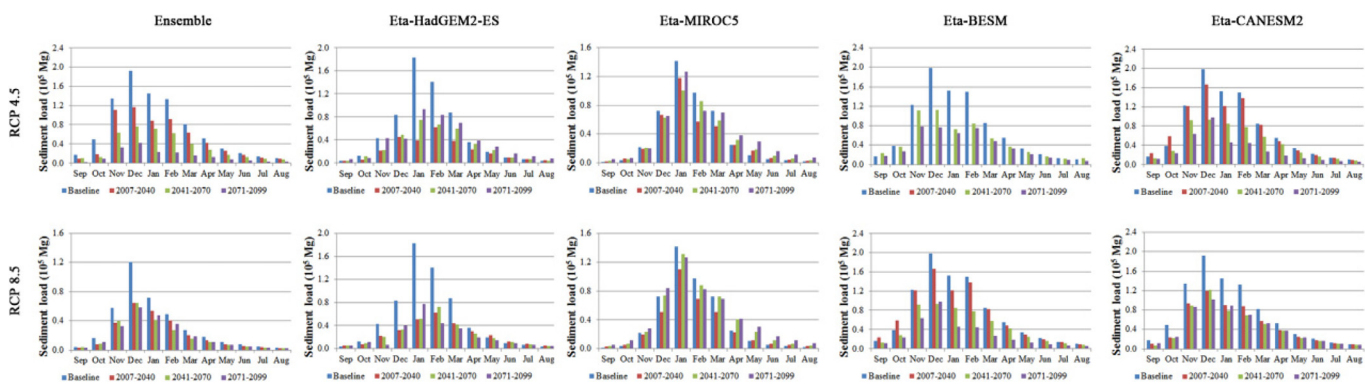


Fig. 10. Mean monthly sediment load projected by the multi-model ensemble and the RCMs Eta-HadGEM2-ES, Eta-MIROC5, Eta-BESM and Eta-CANESM2 for the UPRB under the RCP 4.5 and RCP 8.5.

Table 4

Annual sediment load projections (in 10^5 Mg yr^{-1}) for the multi-model ensemble and the RCMs Eta-HadGEM2-ES, Eta-MIROC5, Eta-BESM and Eta-CANESM2, under the RCPs 4.5 and 8.5. Values between parenthesis represent the percent changes (%).

Model	Scenario	Baseline	2007–2040	2041–2070	2071–2099
Ensemble	RCP 4.5	3.92	2.62 (−33.3)	2.3 (−41.5)	2.34 (−40.3)
	RCP 8.5		2.08 (−47)	1.86 (−52.6)	1.76 (−55.2)
Eta-HadGEM2-ES	RCP 4.5	6.26	2.72 (−56.5)	3.62 (−42.2)	4.48 (−28.4)
	RCP 8.5		3.04 (−51.4)	4.12 (−34.2)	2.73 (−56.4)
Eta-MIROC5	RCP 4.5	4.56	3.77 (−17.3)	4.07 (−10.7)	4.68 (2.6)
	RCP 8.5		3.57 (−21.7)	4.84 (6.2)	5.14 (12.8)
Eta-BESM	RCP 4.5	8.96	—	5.96 (−33.5)	4.7 (−47.5)
	RCP 8.5		8.3 (−7.4)	5.46 (−39.1)	3.66 (−59.1)
Eta-CANESM2	RCP 4.5	8.78	5.83 (−33.6)	5.33 (−39.3)	5.32 (−39.3)
	RCP 8.5		6.02 (−31.4)	4.1 (−53.2)	1.78 (−79.7)

(UPRB), located in Minas Gerais State, Southeast Brazil. The results showed that SWAT was able to predict the streamflow and sediment load adequately.

Regarding the climate change impacts, in general, the simulations from the multi-model ensemble presented intra-annual (monthly) reductions in streamflow varying from 27.6 to 75%. The projections of annual sediment loads indicated the same trends as the streamflow, which varied from −33.3 to 55.2%.

The results of this study showed that, besides all the uncertainties involved in climate change impacts simulations, the Upper Paranaíba River Basin would suffer serious problems regarding to the water availability in extreme climatic conditions such as those simulated by the adopted models. Also, the results of sediment loads indicated that the UPRB may suffer from both positive (reduction of sediment loads) and negative impacts (increase of sediment loads).

Acknowledgements

We would like to thank Dr. Sin Chan Chou on behalf of the National Institute for Space Research – Center for Weather Forecasting and Climate Research (INPE – CPTEC) for providing the climate change projections data.

Funding: This work was supported by the National Council for Scientific and Technological Development – CNPq under the Grant [number 155448/2016-1] and the Foundation for Research of the State of Minas Gerais - FAPEMIG under the Grant [number PM 00415-16].

Appendix A. Supplementary data

Supplementary data to this article can be found online at <https://doi.org/10.1016/j.ecoleng.2019.04.021>.

References

Abbaspour, K.C., Johnson, C.A., Van Genuchten, M.T., 2004. Estimating uncertain flow and transport parameters using a sequential uncertainty fitting procedure. *Vadose Zone J.* 3, 1340–1352. <https://doi.org/10.2113/3.4.1340>.

Abbaspour, K.C., Yang, J., Maximov, I., Siber, R., Bogner, K., Mieleitner, J., Zobrist, J., Srinivasan, R., 2007. Modelling hydrology and water quality in the pre-alpine/alpine Thur watershed using SWAT. *J. Hydrol.* 333, 413–430. <https://doi.org/10.1016/j.jhydrol.2006.09.014>.

Agência Nacional de Águas (ANA), Plano de recursos hídricos e do enquadramento dos corpos hídricos superficiais da bacia hidrográfica do rio Paranaíba, 2013, Brasília.

Alexander, M.A., Scott, J.D., Mahoney, K., Barsugli, J., 2013. Greenhouse gas – induced changes in summer precipitation over Colorado in NARCCAP regional climate models*. *J. Clim.* 26, 8690–8697. <https://doi.org/10.1175/JCLI-D-13-00088.1>.

Allen, R.G., Pereira, L.S., Raes, D., Smith, M., 1998. Crop evapotranspiration: Guidelines for computing crop water requirements. FAO Irrigation and Drainage Paper 56, Rome, Italy.

Araújo, F.S., Salviano, A.A.C., Neto, M.R.H., 2011. Estimativa da Erodibilidade de Latossolos do Piauí. *Sci. Plena* 7, 1–6.

Arnold, J.G., Srinivasan, R., Muttiyah, R.S., Williams, J.R., 1998. Large area hydrologic modeling and assessment part I: model development. *J. Am. Water Resour. Assoc.* 34, 73–89. <https://doi.org/10.1111/j.1752-1688.1998.tb05961.x>.

Beskow, S., Timm, L.C., Emanuel, V., Tavares, Q., 2016. Potential of the LASH model for water resources management in data-scarce basins: a case study of the Fraga River basin, southern Brazil. *Hydrol. Sci. J.* 61, 2567–2578. <https://doi.org/10.1080/02626667.2015.1133912>.

Beven, K., Binley, A., 1992. The future of distributed models: model calibration and uncertainty prediction. *Hydrol. Process.* 6, 279–298. <https://doi.org/10.1002/hyp.3360060305>.

Castro, W.J., Lemke-de-Castro, M.L., Lima, J.O., Oliveira, L.F.C., Rodrigues, C., Figueiredo, C.C., 2011. Erodibilidade de Solos do Cerrado Goiano. *Rev. Agronegócios e Meio Ambiente*. 4, 305–320.

Chen, J., Brissette, P., Chaumont, D., Braun, M., 2013. Finding appropriate bias correction methods in downscaling precipitation for hydrologic impact studies over North America. 49, 4187–4205. <https://doi.org/10.1002/wrcr.20331>.

Chou, S.C., Lyra, A., Mourão, C., Dereczynski, C., Pilotto, I., Gomes, J., Bustamante, J., Tavares, P., Silva, A., Rodrigues, D., Campos, D., Chagas, D., Sueiro, G., Siqueira, G., Marengo, J., 2014a. Assessment of climate change over South America under RCP 4.5 and 8.5 downscaling scenarios. *Am. J. Clim. Chang.* 3, 512–525. <https://doi.org/10.4236/ajcc.2014.35043>.

Chou, S.C., Lyra, A., Mourão, C., Dereczynski, C., Pilotto, I., Gomes, J., Bustamante, J., Tavares, P., Silva, A., Rodrigues, D., Campos, D., Chagas, D., Sueiro, G., Siqueira, G., Nobre, P., Marengo, J.A., 2014b. Evaluation of the Eta simulations nested in three global climate models. *Am. J. Clim. Chang.* 3, 438–454. <https://doi.org/10.4236/ajcc.2014.35039>.

Cousino, L.K., Becker, R.H., Zmijewski, K.A., 2015. Modeling the effects of climate change on water, sediment, and nutrient yields from the Maumee River watershed. *J. Hydrol. Reg. Stud.* 4, 762–775. <https://doi.org/10.1016/j.ejrh.2015.06.017>.

de Oliveira, V.A., de Mello, C.R., Viola, M.R., Srinivasan, R., 2017. Assessment of climate change impacts on streamflow and hydropower potential in the headwater region of the Grande river basin, Southeastern Brazil. *Int. J. Climatol.* 37, 5005–5023. <https://doi.org/10.1002/joc.5138>.

de Oliveira, V.A., Mello, C.R., Durães, M.F., Silva, A.M., 2014. Soil erosion vulnerability in the Verde River Basin. *Southern Minas Gerais Ciência & Agrotecnologia* 38, 262–269. <https://doi.org/10.1590/S1413-70542014000300006>.

Dlamini, N.S., Kamal, R., Amin, M., Mohd, B., Syazwan, M., Fikri, A., Abdullah, B., Hin, L.S., 2017. Modeling potential impacts of climate change on streamflow using projections of the 5th assessment report for the Bernam River Basin, Malaysia. *Water* 9, 226. <https://doi.org/10.3390/w9030226>.

Durães, M.F., Coelho Filho, J.A.P., de Oliveira, V.A., 2016. Water erosion vulnerability and sediment delivery rate in upper Iguaçu river basin – Paraná. *Brazilian J. Water Resour.* 21, 728–741. <https://doi.org/10.1590/2318-0331.011616029>.

Ferreira, L.G., Urban, T.J., Neuenschwander, A., Araújo, F.M., 2011. Use of Orbital LIDAR in the Brazilian cerrado biome: potential applications and data availability. *Remote Sens.* 3, 2187–2206. <https://doi.org/10.3390/rs3102187>.

Fiseha, B.M., Setegn, S.G., Melesse, A.M., Volpi, E., Fiori, A., 2014. Impact of climate change on the hydrology of upper tiber river basin using bias corrected regional climate model. *Water Resour. Manag.* 28, 1327–1343. <https://doi.org/10.1007/s11269-014-0546-x>.

Fowler, H.J., Ekström, M., 2009. Multi-model ensemble estimates of climate change impacts on UK seasonal precipitation extremes. *Int. J. Climatol.* 416, 385–416. <https://doi.org/10.1002/joc>.

Fowler, H.J., Ekström, M., Blenkinsop, S., Smith, A.P., 2007. Estimating change in extreme European precipitation using a multimodel ensemble. *J. Geophys.* 112, D18104. <https://doi.org/10.1029/2007JD008619>.

Fundação Estadual do Meio Ambiente (FEAM), 2010. *Mapa de Solos do Estado de Minas Gerais*, first ed. Fundação Estadual do Meio Ambiente, Belo Horizonte.

Graham, L.P., Andréasson, J., Carlsson, B., 2007. Assessing climate change impacts on hydrology from an ensemble of regional climate models, model scales and linking methods – a case study on the Lule River basin. *Clim. Change* 81, 293–307. <https://doi.org/10.1007/s10584-006-9215-2>.

Green, W.H., Ampt, G.A., 1911. Studies on soil physics, 1. The flow of air and water through soils. *J. Agric. Sci.* 4, 11–24.

Hargreaves, G.L., Hargreaves, G.H., Riley, J.P., 1985. Agricultural benefits for senegal river basin. *J. Irrig. Drain. Eng.* 111, 113–124.

Intergovernmental Panel on Climate Change. 2013. Climate change 2013: The physical science basis. Contribution of Working Group I to the Fifth Assessment Report of the Intergovernmental Panel on Climate Change, 2013. Cambridge University Press, Cambridge.

Jackson, W.L., Gebhardt, K., Van Haveren, B.P., 1986. Use of the modified universal soil

loss equation for average annual sediment yield estimates on small rangeland drainage basins. *Drainage basin sediment delivery. Proc. Symposium, Albuquerque*, pp. 413–422.

Jiang, T., Yongqin, C.D., Xu, C., Chen, X., Chen, X., Singh, V.P., 2007. Comparison of hydrological impacts of climate change simulated by six hydrological models in the Dongjiang Basin, South China. *J. Hydrol.* 336, 316–333. <https://doi.org/10.1016/j.jhydrol.2007.01.010>.

Johnson, C.W., Gordon, N.D., Hanson, C.L., 1986. North-west rangeland sediment yield analysis by the MUSLE. *Trans. Am. Soc. Agric. Biol. Eng.* 26, 1889–1895.

Lemann, T., Zeleke, G., Amsler, C., Giovanoli, L., Suter, H., Roth, V., 2016. Modelling the effect of soil and water conservation on discharge and sediment yield in the upper Blue Nile basin. *Ethiopia. Appl. Geogr.* 73, 89–101. <https://doi.org/10.1016/j.apgeog.2016.06.008>.

Lenderink, G., Buishand, A., Deursen, W. Van, 2007. Estimates of future discharges of the river Rhine using two scenario methodologies: direct versus delta approach. *Hydrolog. Earth Syst. Sci.* 11, 1145–1159. <https://doi.org/10.5194/hess-11-1145-2007>.

Li, Z., Xu, X., Yu, B., Xu, C., Liu, M., Wang, K., 2016. Quantifying the impacts of climate and human activities on water and sediment discharge in a karst region of southwest China. *J. Hydrol.* 542, 836–849. <https://doi.org/10.1016/j.jhydrol.2016.09.049>.

Ma, X., Lu, X.X., Noordwijk, M. Van, Li, J.T., Xu, J.C., 2014. Attribution of climate change, vegetation restoration, and engineering measures to the reduction of suspended sediment in the Kejire catchment, southwest China. *Hydrolog. Earth Syst. Sci.* 18, 1979–1994. <https://doi.org/10.5194/hess-18-1979-2014>.

Mannigel, A.R., Carvalho, M.P., Moretti, D., Medeiros, L.R., 2002. Fator erodibilidade e tolerância da perda dos solos do Estado de São Paulo. *Acta Scientiarum.* 24, 1335–1340. <https://doi.org/10.4025/actasciagron.v24i0.2374>.

Mello, C.R., Viola, M.R., Norton, L., Silva, A.M., Weimar, F.S., 2008. Development and application of a simple hydrologic model simulation for a Brazilian headwater basin. *Catena* 75, 235–247. <https://doi.org/10.1016/j.catena.2008.07.002>.

Milliman, J.D., Farnsworth, K.J., Jones, P.D., Xu, K.H., Smith, L.C., 2008. Climatic and anthropogenic factors affecting river discharge to the global ocean, 1951–2000. *Glob. Planet. Change* 62, 187–194. <https://doi.org/10.1016/j.gloplacha.2008.03.001>.

Mohor, G.S., Rodriguez, D.A., Tomasella, J., Siqueira Júnior, J.L., 2015. Exploratory analyses for the assessment of climate change impacts on the energy production in an Amazon run-of-river hydropower plant. *J. Hydrol. Reg. Stud.* 4, 41–59. <https://doi.org/10.1016/j.ejrh.2015.04.003>.

Molina-Navarro, E., Hallack-Alegria, M., Martínez-Pérez, S., Ramírez-Hernández, J., Mungaray-Moctezuma, A., Sastre-Merlín, A., 2015. Hydrological modeling and climate change impacts in an agricultural semiarid region. Case study: Guadalupe River basin, Mexico. *Agric. Water Manag.* 175, 29–42. <https://doi.org/10.1016/j.agwat.2015.10.029>.

Moriasi, D.N., Arnold, J.G., Van Liew, M.W., Bingner, R.L., Harmel, R.D., Veith, T.L., 2007. Model evaluation guidelines for systematic quantification of accuracy in watershed simulations. *Trans. ASABE* 50, 885–900. <https://doi.org/10.13031/2013.23153>.

Myers, N., Mittermeier, R.A., Mittermeier, C.G., da Fonseca, G.A.B., Kent, J., 2000. Biodiversity hotspots for conservation priorities. *Nature* 403, 853–858. <https://doi.org/10.1038/35002501>.

Naik, P.K., Jay, D.A., 2011. Distinguishing human and climate influences on the Columbia River: Changes in mean flow and sediment transport. *J. Hydrol.* 404, 259–277. <https://doi.org/10.1016/j.jhydrol.2011.04.035>.

Nash, J.E., Sutcliffe, J.V., 1970. River flow forecasting through conceptual models: a discussion of principles. *J. Hydrol.* 10, 282–290.

Neitsch, S.L., Arnold, J.G., Kiniry, J.R., Williams, J.R., 2005. Soil and water assessment tool theoretical documentation. Temple.

Ouyang, F., Zhu, Y., Fu, G., Lü, H., Zhang, A., Yu, Z., Chen, X., 2015. Impacts of climate change under CMIP5 RCP scenarios on streamflow in the Huangnizhuang catchment. *Stoch. Environ. Res. Risk Assess.* 29, 1781–1795. <https://doi.org/10.1007/s00477-014-1018-9>.

Parajuli, P.B., Jayakody, P., Sassenrath, G.F., Ouyang, Y., 2016. Assessing the impacts of climate change and tillage practices on stream flow, crop and sediment yields from the Mississippi River Basin. *Agric. Water Manag.* 168, 112–124. <https://doi.org/10.1016/j.agwat.2016.02.005>.

Pesquero, J.F., Chou, S.C., Nobre, C.A., Marengo, J.A., 2009. Climate downscaling over South America for 1961–1970 using the Eta Model. *Theor. Appl. Climatol.* 99, 75–93. <https://doi.org/10.1007/s00704-009-0123-z>.

Phan, D.B., Wu, C.C., Hsieh, S.C., 2011. Impact of climate change on stream discharge and sediment yield in Northern Viet Nam. *Water Resour.* 38, 827–836. <https://doi.org/10.1134/S0097807811060133>.

Priestley, C.H.B., Taylor, R.J., 1972. On the assessment of surface heat flux and evaporation using large-scale parameters. *Month. Weath. Rev.* 100, 81–92.

Projeções de mudança do clima para a América do Sul regionalizadas pelo modelo Eta (PROJETA), 2018. <https://projeta.cptec.inpe.br>. Accessed: 10 jul 2018.

Prudhomme, C., Davies, H., 2009. Assessing uncertainties in climate change impact analyses on the river flow regimes in the UK. Part 2: Future climate. *Clim. Change* 93, 197–222. <https://doi.org/10.1007/s10584-008-9461-6>.

Ribeiro Neto, A., Rolim, A., Marengo, J.A., Chou, S.C., 2016. Hydrological processes and climate change in hydrographic regions of Brazil. *J. Water Resour. Prot.* 8, 1103–1127. <https://doi.org/10.4236/jwarp.2016.812087>.

Rodríguez-Blanco, M.L., Arias, R., Taboada-Castro, M.M., Nunes, J.P., Keizer, J.J., Taboada-Castro, M.T., 2016. Potential impact of climate change on suspended sediment yield in NW Spain: A case study on the corbeira catchment. *Water* 8, 444. <https://doi.org/10.3390/w8100444>.

Sano, E.E., Rosa, R., Brito, J.L.S., Ferreira, L.G., 2010. Land cover mapping of the tropical savanna region in Brazil. *Environ. Monit. Assess.* 166, 113–124. <https://doi.org/10.1007/s10661-009-0988-4>.

Setegn, S.G., Dargahi, B., Srinivasan, R., Melesse, A.M., 2010. Modeling of sediment yield from Anjeni-Gauged watershed, Ethiopia using SWAT model. *J. Am. Water Resour. Assoc.* 46, 514–526. <https://doi.org/10.1111/j.1752-1688.2010.00431.x>.

Shamir, E., Megdal, S.B., Carrillo, C., Castro, C.L., Chang, H.I., Chief, K., Corkhill, F.E., Eden, S., Georgakakos, K.P., Nelson, K.M., Pietro, J., 2015. Climate change and water resources management in the Upper Santa Cruz River, Arizona. *J. Hydrol.* 521, 18–33. <https://doi.org/10.1016/j.jhydrol.2014.11.062>.

Shrestha, B., Babel, M.S., Maskey, S., van Griensven, A., Uhlenbrook, S., Green, A., Akkharath, I., 2013. Impact of climate change on sediment yield in the Mekong River basin: a case study of the Nam Ou basin. *Lao PDR. Hydrol. Earth Syst. Sci.* 17, 1–20. <https://doi.org/10.5194/hess-17-1-2013>.

Shrestha, B., Cochrane, T.A., Caruso, B.S., Arias, M.E., Piman, T., 2016. Uncertainty in flow and sediment predictions due to future climate scenarios for the 3S Rivers in the Mekong Basin. *J. Hydrol.* 540, 1088–1104. <https://doi.org/10.1016/j.jhydrol.2016.07.019>.

Srinivasan, R., Ranabarayanan, T.S., Arnold, J.G., Bednarz, S.T., 1998. Large area hydrologic modeling and assessment part II: model application. *J. Am. Water Resour. Assoc.* 34, 91–101. <https://doi.org/10.1111/j.1752-1688.1998.tb05962.x>.

Srinivasan, R., Zhang, Z., Arnold, J.G., 2010. SWAT ungauged: hydrological budget and crop yield predictions in the upper Mississippi river basin. *Trans. ASABE* 53, 1533–1546. <https://doi.org/10.13031/2013.34903>.

Tang, L., Yang, D., Hu, H., Gao, B., 2011. Detecting the effect of land-use change on streamflow, sediment and nutrient losses by distributed hydrological simulation. *J. Hydrol.* 409, 172–182. <https://doi.org/10.1016/j.jhydrol.2011.08.015>.

Teutschbein, C., Seibert, J., 2012. Bias correction of regional climate model simulations for hydrological climate-change impact studies: review and evaluation of different methods. *J. Hydrol.* 456–457, 12–29. <https://doi.org/10.1016/j.jhydrol.2012.05.052>.

Teutschbein, C., Seibert, J., 2010. Regional climate models for hydrological impact studies at the catchment scale: a review of recent modeling strategies. *Geogr. Compass* 4, 834–860. <https://doi.org/10.1111/j.1749-8198.2010.00357.x> Regional.

Tomkins, K.M., 2014. Uncertainty in streamflow rating curves: methods, controls and consequences. *Hydrolog. Process.* 28, 464–481. <https://doi.org/10.1002/hyp.9567>.

Trenberth, K.E., Miller, K., Mearns, L., Rhodes, S., 2000. Effects of Changing Climate on Weather and Human Activities. University Science Books, Sausalito.

United States Department of Agriculture – Soil Conservation Service (USDA-SCS), 1972. National Engineering Handbook, Section 4 Hydrology, Chapters 4–10.

van Griensven, A., Bauwens, W., 2003. Multiobjective autocalibration for semidistributed water quality models. *Water Resour. Res.* 39, 1–9. <https://doi.org/10.1029/2003WR002284>.

Vetter, T., Reinhardt, J., Flörke, M., van Griensven, A., Hattermann, F., Huang, S., Koch, H., Pechlivanidis, I.G., Plötner, S., Seidou, O., Su, B., Vervoort, R.W., Krysanova, V., 2017. Evaluation of sources of uncertainty in projected hydrological changes under climate change in 12 large-scale river basins. *Clim. Change* 141, 419–433. <https://doi.org/10.1007/s10584-016-1794-y>.

Viola, M.R., de Mello, C.R., Chou, S.C., Yanagi, S.N., Gomes, J.L., 2014. Assessing climate change impacts on Upper Grande River Basin hydrology, Southeast Brazil. *Int. J. Climatol.* 35, 1054–1068. <https://doi.org/10.1002/joc.4038>.

Williams, J.R., 1995. The EPIC Model. In: Singh, V.P. (Ed.), *Computer Models of Watershed Hydrology*. Water Resources Publications, pp. 909–1000.

Yan, B., Fang, N.F., Zhang, P.C., Shi, Z.H., 2013. Impacts of land use change on watershed streamflow and sediment yield: an assessment using hydrologic modeling and partial least squares regression. *J. Hydrol.* 484, 26–37. <https://doi.org/10.1016/j.jhydrol.2013.01.008>.

Zeiger, S.J., Hubbart, J.A., 2016. Science of the Total Environment A SWAT model validation of nested-scale contemporaneous stream flow, suspended sediment and nutrients from a multiple-land-use watershed of the central USA. *Sci. Total Environ.* 572, 232–243. <https://doi.org/10.1016/j.scitotenv.2016.07.178>.

Zhang, Y., Su, F., Hao, Z., Xu, C., Yu, Z., Wang, L., Tong, K., 2015. Impact of projected climate change on the hydrology in the headwaters of the Yellow River basin. *Hydrolog. Process.* 29, 4379–4397. <https://doi.org/10.1002/hyp.10497>.

Zhao, Y., Zou, X., Gao, J., Xu, X., Wang, C., Tang, D., Wang, T., Wu, X., 2015. Quantifying the anthropogenic and climatic contributions to changes in water discharge and sediment load into the sea: a case study of the Yangtze River. *China. Sci. Total Environ.* 536, 803–812. <https://doi.org/10.1016/j.scitotenv.2015.07.119>.